Thermodynamics of Sequence-Specific Glucocorticoid Receptor–DNA Interactions†

Thomas Lundbäck,‡ Johanna Zilliacus,§ Jan-Åke Gustafsson,⊥ Jan Carlstedt-Duke,⊥ and Torleif Härd*,‡

Centers for Structural Biochemistry and Biotechnology and Department of Medical Nutrition, Karolinska Institutet, NOVUM, S-141 57 Huddinge, Sweden

Received October 18, 1993; Revised Manuscript Received January 26, 1994®

ABSTRACT: The thermodynamics of sequence-specific DNA–protein interactions provide a complement to structural studies when trying to understand the molecular basis for sequence specificity. We have used fluorescence spectroscopy to study the chemical equilibrium between the wild-type and a triple mutant glucocorticoid receptor DNA-binding domain (GR DBD_{wt} and GR DBD_{EGA}, respectively) and four related DNA-binding sites (response elements). NMR spectroscopy was used to confirm that the structure of the two proteins is very similar in the uncomplexed state. Binding to DNA oligomers containing single half-sites and palindromic binding sites was studied to obtain separate determinations of association constants and cooperativity parameters involved in the dimeric DNA binding. Equilibrium parameters were determined at 10–35 °C in 85 mM NaCl, 100 mM KCl, 2 mM $MgCl_2$, and 20 mM Tris-HCl at pH 7.4 (20 °C) and at low concentrations of an antioxidant and a nonionic detergent. GR DBD_{wt} binds preferentially to a palindromic consensus glucocorticoid response element (GRE) with an association constant of $(7.6 \pm 0.9) \times 10^5$ M^{-1} and a cooperativity parameter of 10 ± 1 at 20 °C. GR DBD_{EGA} has the highest affinity for an estrogen response element (ERE) with an association constant of $(2.2 \pm 0.3) \times 10^5$ M^{-1} and a cooperativity parameter of 121 ± 17 at 20 °C. The difference in cooperativity in the two binding processes, which indicates significant differences in binding modes, was confirmed using gel mobility shift assays. van't Hoff analysis shows that DNA binding in all cases is entropy driven within the investigated temperature range. We find that $\Delta H°_{obs}$ and $\Delta S°_{obs}$ for the formation of a GR DBD_{wt}–GRE versus GR DBD_{EGA}–ERE complex are significantly different despite very similar $\Delta G°_{obs}$ values. A comparison of GR DBD_{wt} binding to two similar GREs reveals that the discrimination between these two (specific) sites is due to a favorable $\Delta(\Delta S°_{obs})$ which overcompensates an unfavorable $\Delta(\Delta H°_{obs})$, i.e., the sequence specificity is in this case entropy driven. Thus, entropic effects are of decisive importance for the affinity as well as the specificity in GR–DNA interactions. The molecular basis for measured equilibrium and thermodynamic parameters is discussed on the basis of published structures of GR DBD–GRE and ER DBD–ERE complexes.

The glucocorticoid receptor (GR)[1] is a member of the intracellular nuclear receptor superfamily of ligand-inducible transcription factors, which also includes receptors for other steroid hormones (such as the estrogen receptor, ER), thyroid hormone, retinoic acids, vitamin D_3, and several orphan receptors with unidentified ligands or activation mechanisms [see reviews by Evans (1988), Beato (1989), and Parker (1991)]. The various receptors within the superfamily have three major functional domains—an N-terminal domain involved in transactivation, a central DNA-binding domain, and a C-terminal ligand-binding domain. The ligand-activated receptor binds to specific DNA sequences, hormone response elements, located close to regulated genes and activates or inhibits gene transcription.

The GR binds preferentially to the glucocorticoid response element (GRE), which is a partially palindromic sequence (Figure 1, bottom) comprising two hexameric half-sites with an intervening sequence of three base pairs (Beato, 1989). The half-sites are arranged as inverted repeats, and the GR binds to the GRE as a dimer with one protein molecule contacting each half-site (Luisi et al., 1991; Tsai et al., 1988). Protein fragments containing the glucocorticoid receptor DNA-binding domain (GR DBD) expressed in *Escherichia coli* are monomeric (Härd et al., 1990b,c) in the uncomplexed state but bind cooperatively to form a dimeric complex on a GRE (Dahlman-Wright et al, 1990; Härd et al., 1990a). [See Härd and Gustafsson (1993) for a review on the structure and function of steroid receptor DNA-binding domains.] The GR DBD is able to discriminate between the GRE and an estrogen response element (ERE), although the two response elements differ in only one or two central base pairs per half-site (Klock et al., 1987; Strähle et al., 1987). Three amino acid residues (G458, S459, and V462 in the rat GR; Figure 1, top) in the recognition helix of the GR and ER DBDs have been identified as primarily responsible for the discrimination between a GRE and an ERE (Danielsen et al., 1989; Mader et al., 1989; Umesono & Evans, 1989). The exchange of these residues in the GR DBD for the corresponding residues in the ER DBD results in an altered specificity of the mutant protein (Zilliacus et al., 1991). A comparison of the GR DBD–GRE structure with a recently determined ER DBD–ERE structure (Schwabe et al., 1993) shows that the origin of sequence specificity is not a simple matter of exchanging functional groups on interacting surfaces within an otherwise fixed

† This work was supported by the Swedish Natural Sciences Research Council (Grants No. K-KU 8593-309 and No. S-FO 8593-308), the Magn. Bergvall Foundation, the Swedish Medical Research Council (Grants No. 2819 and No. 8998), and the Swedish Research Council for Engineering Sciences.

* Author to whom correspondence should be addressed. Telephone: +46 8 608 92 30. Fax: +46 8 608 92 90.

‡ Center for Structural Biochemistry.

§ Center for Biotechnology.

⊥ Department of Medical Nutrition.

® Abstract published in *Advance ACS Abstracts,* April 15, 1994.

[1] Abbreviations: GR, glucocorticoid receptor; GRE, glucocorticoid response element; ER, estrogen receptor; ERE, estrogen response element; DBD, DNA-binding domain; bp, base pair; DTT, dithiothreitol; $C_{12}E_8$, octaethylene glycol monododecyl ether; PMSF, phenylmethanesulfonyl fluoride; NMR, nuclear magnetic resonance; NOESY, 2-dimensional nuclear Overhauser enhancement spectroscopy; TOCSY, 2-dimensional total correlation spectroscopy.

0006-2960/94/0433-5955$04.50/0

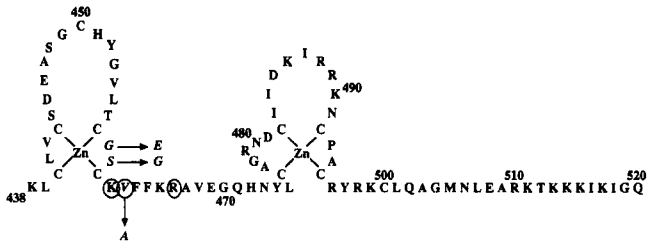

		1 2 3 4 5 6
palGRE	AGAACA TGA	TGTTCT
palGRE2	AGGACA TGA	TGTCCT
palERE2	AGATCA TGA	TGATCT
palERE	AGGTCA TGA	TGACCT
GREH		TGTTCT
GRE2H		TGTCCT
ERE2H		TGATCT
EREH		TGACCT
GREX		GGCATG

FIGURE 1: (Top) Amino acid sequence of the rat GR DBD_{wt}. Arrows show the amino acid residues introduced into the mutant GR DBD_{EGA} with an altered DNA-binding specificity. Indicated in circles are the amino acid residues making specific DNA base contacts in the X-ray structure of the GR DBD–GRE complex (Luisi et al., 1991). (Bottom) Sequences of response elements studied. The hexameric GREH and EREH half-sites differ in two central base pairs (positions 3 and 4), while GRE2H and ERE2H are the corresponding intermediate half-sites. A nonspecific sequence at the half-site position (GREX) was also included in the studies. The palGRE, palGRE2, palERE2, and palERE are idealized response elements with two half-sites arranged as inverted repeats. All sequences are incorporated in DNA oligomers as described under Materials and Methods.

structural framework, despite the high similarities in protein structures and DNA-binding site sequences. Furthermore, our previous studies on a series of mutant GR DBDs suggested that some of the discriminatory properties result from inhibition of binding to noncognate sites (Zilliacus et al., 1992). Clearly, additional structural information as well as a characterization of the thermodynamics of complex formation is necessary to understand the molecular basis for DNA sequence discrimination by the GR and ER DBDs.

Specific interactions between functional groups on the interacting surfaces observed in structures of DNA–protein complexes determined by crystallography or NMR are often considered to contribute to the enthalpy component of the free energy of the association process. On the other hand, several lines of evidence suggest that entropic factors might contribute significantly and the formation of DNA–protein complexes are often found to be entropy driven, at least within certain temperature ranges (Ha et al., 1989; Record, Jr. et al., 1991; Takeda et al., 1992; Brenowitz et al., 1990; Botuyan et al., 1993; Lundbäck et al., 1993). However, these observations are not necessarily contradictory since sequence specificity might be achieved through enthalpy differences in association processes that are entropy driven.

The issues of DNA–protein interactions in general and the sequence-specific DNA binding of the GR DBD in particular have motivated us to undertake a series of studies of the GR DBD–DNA equilibrium using fluorescence spectroscopy. These studies are clearly complementary to the gel mobility shift assays mentioned above but more detailed in that various equilibrium parameters can be quantitatively determined. Furthermore, enthalpic and entropic contributions to the free energy of binding can be estimated by means of van't Hoff analysis. In an initial paper, we reported on the dimeric cooperative binding of the GR DBD to a GRE sequence and the relative affinities for nonspecific and specific DNA sequences at various salt concentrations (Härd et al., 1990a). In a second paper, the relative affinities for GR DBD to various GRE and ERE half-sites and a palindromic GRE sequence were studied. The temperature dependence for GR DBD binding to a GRE half-site also revealed the thermodynamic fingerprint of the hydrophobic effect, i.e., a large negative change in specific heat capacity, resulting in compensating enthalpic and entropic components of the free energy of association (Lundbäck et al., 1993).

In the present work, we study the thermodynamics of DNA binding by the wild-type GR DBD (GR DBD_{wt}) and a triple mutant GR DBD (GR DBD_{EGA}), where the three amino acids that are responsible for the discrimination between GREs and EREs have been replaced by the corresponding amino acids of the ER. The relative affinities of these proteins to a series of related half-site and palindromic GRE and ERE sequences are measured, and the thermodynamics of binding are analyzed for the strongest complexes. The results enable us to quantify the thermodynamic origins of sequence-specific DNA binding of the two proteins to various response elements.

MATERIALS AND METHODS

Protein Purification. The wild-type GR DBD_{wt} (equal to the segment K438–Q520 of the rat GR and the segment K419–Q501 of the human GR) and the corresponding mutant GR DBD_{EGA} were overexpressed using the plasmid pT7-7 in the *E. coli* strain BL21[DE]/pLysS. The mutant GR DBD_{EGA} is a GR DBD with residues G439, S440, and V443 mutated to the corresponding residues (E, G, and A, respectively) in the ER (Zilliacus et al., 1991). The bacteria were grown at 37 °C in Luria broth medium containing 1% casamino acids, 1% glucose, 100 μg/mL ampicillin, and 30 μg/mL chloramphenicol to $A_{600} = 0.6$. Protein expression was induced with 0.2 mM isopropyl β-D-thiogalactopyranoside (IPTG) for 2 h. The cells were resuspended in lysis buffer (50 mM Tris-HCl at pH 7.5, 1 mM EDTA, 0.5 M NaCl, 10% glycerol, 1 mM dithiothreitol (DTT), 1 mM phenylmethanesulfonyl fluoride (PMSF), 1 μg/mL leupeptin, 10 μg/mL trypsin inhibitor), and deoxycholic acid was added to a final concentration of 0.05%. The lysate was centrifuged at 39000*g* for 30 min. Polyethyleneimine was added to the clarified lysate to a final concentration of 0.2%, and the nucleic acid precipitate was removed by centrifugation at 39000*g* for 30 min. The lysate was then treated with ammonium sulfate at 70% saturation. The precipitate was collected by centrifugation, resuspended in 50 mM Tris-HCl at pH 8.0, 50 mM NaCl, 1 mM EDTA, 5 mM DTT, 1 mM $ZnSO_4$, 1 mM PMSF, 1 μg/mL leupeptin, and 10 μg/mL trypsin inhibitor, and dialyzed against the same buffer. The dialyzed lysate was loaded onto a CM-Sepharose column (Pharmacia) and eluted with a linear NaCl gradient (125–800 mM for GR DBD_{wt} and 125–300 mM for GR DBD_{EGA}) in 20 mM phosphate buffer at pH 7.6 with 1 mM DTT. The eluted protein was loaded onto a HiLoad Superdex 75 prep grade FPLC column (Pharmacia) and eluted with 20 mM phosphate buffer at pH 7.6 with 150 mM NaCl and 1 mM DTT. After elution, the protein was dialyzed against a buffer containing 50 mM Tris-HCl at pH 7.4, 50 mM NaCl, and 1 mM DTT for storage. The protein was >95% pure as estimated from SDS polyacrylamide gels stained by Coomassie Blue R 250. Protein stock concentrations were

determined spectrophotometrically using the extinction coefficient ϵ_{280nm} = 4200 M^{-1} cm^{-1} calculated for tyrosine absorption (Cantor & Schimmel, 1980).

Synthesis and Purification of DNA. Synthetic DNA oligomers were used for equilibrium studies of specific binding and for gel mobility shift assays. The single half-site sequences and the palindromic binding sequences (Figure 1, bottom) were incorporated in 32-base pair (bp) (CCTAGAGGATCTGAXXXXXXAGATCGAATTCG) and 41-bp (GACCCTAGAGGATXXXXXXTGAXXXXXXAGATCGAATTCG) oligomers, respectively, in which the hexameric X-sequence represents the binding sites. The GRE, GRE2, and ERE half-sites are all consensus sequences of naturally occurring response elements, whereas the ERE2 sequence was included for completeness. A nonspecific sequence at the half-site position (GREX) was also included in the studies. All DNA oligomers were purified using high-pressure liquid chromatography. Following purification, complementary strands were annealed by heating at 75 °C for 10 min and then slowly cooled to room temperature in 150 mM NaCl and 10 mM Tris-HCl at pH 7.4. All DNA concentrations were determined spectrophotometrically using an average extinction coefficient ϵ_{260nm} = 13 200 M bp^{-1} cm^{-1} (Mahler et al., 1964).

Gel Mobility Shift Assays. The oligonucleotides were labeled with [γ-^{32}P]ATP using polynucleotide kinase and separated from unincorporated oligomers using a NICK column (Pharmacia). Labeled oligonucleotide (0.01 pmol, 0.3 ng) was incubated with 0.4 pmol (3 ng) or 0.7 pmol (6 ng) of purified protein for 30 min at room temperature in 10 μL of buffer containing 10 mM HEPES at pH 7.5, 10% glycerol, 2.5 mM $MgCl_2$, 50 mM KCl, 0.1 mM EDTA, and 1 mM DTT. Protein–DNA complexes were separated from protein-free DNA by nondenaturing gel electrophoresis (Fried & Crothers, 1981) in 5% polyacrylamide (29:1, acrylamide: bisacrylamide) gels at 4 °C. Gels were run at a constant voltage of 200 V, dried, and exposed to Kodak XAR-5 film.

NMR Spectroscopy. NMR samples of GR DBD_{wt} and GR DBD_{EGA} contained approximately 1 mM protein in 10% D_2O, 50 mM NaCl, 1 mM DTT, and 10 mM phosphates at pH 7.5. NMR spectra were recorded on a Varian Unity 500 spectrometer at a magnetic field of 11.74 T. NOESY spectra (Macura & Ernst, 1980), with mixing times of 150 ms, and "clean" TOCSY spectra (Griesinger et al., 1988), with mixing times of 60 ms, were recorded at 26 °C. These spectra were sufficient for sequential assignment of the GR DBD_{EGA} ^{1}H NMR spectrum and comparison of GR DBD_{EGA} to GR DBD_{wt} with regard to secondary structure elements, etc. The recording of 2D NMR spectra and processing, etc., were carried out as in the NMR analysis of GR DBD, which has been extensively described elsewhere (Härd et al., 1990b,c; Berglund et al., 1992; Baumann et al., 1993).

Equilibrium Titrations. Fluorescence measurements were carried out on a Shimadzu RF-5000 spectrofluorophotometer equipped with a 150-W xenon arc lamp. A Hellma 104F-QS quartz cell in combination with a Hellma Cuv-O-Stir Model 333 and a small magnetic stir bar placed in the cuvette were used in order to allow efficient mixing during titrations. The temperature of the cell compartment was controlled using a Shimadzu constant-temperature cell holder connected to a Hetofrig CB IIe circulating water bath. The temperature in the cuvette was measured using a thermoelement connected to a TsT 420 digital thermometer and could be controlled with a precision of ±0.2 °C.

Equilibrium titrations were carried out in a buffer containing 85 mM NaCl, 100 mM KCl, 2 mM $MgCl_2$, 0.3 mM DTT, 0.1 mM octaethylene glycol monododecyl ether ($C_{12}E_8$), and 20 mM Tris-HCl at pH 7.4 (20 °C).

Titrations were performed as reverse titrations, in which different amounts of DNA were added at a constant protein concentration. Samples were at all times allowed to reach thermal equilibrium in the cuvette. The titrant was added using a microsyringe with a repeating adapter, and the emission spectrum was recorded three times in order to minimize the effects of instrumental fluctuations. The excitation wavelength was 280 nm and the fluorescence intensities used for calculating binding isotherms were sampled with 0.2-nm intervals within the emission wavelength range 304–307 nm. Measured fluorescence intensities were corrected for background emission and Raman light scattering from water by subtracting signals from DNA + buffer samples obtained in blank titrations at 20 °C and for optical filtering effects (Birdsall et al., 1983) due to DNA absorption at 280 nm. The temperature dependencies of DNA absorption and background signals were measured and corrected for. The excitation shutter was closed between measurements as a precaution to photochemical degradation of the protein. However, no photobleaching could be observed within the time corresponding to a complete titration even under continuous illumination.

The fractional fluorescence quenching (Q_{obsd}) was calculated as $(I_o - I)/I_o$, where I_o is the protein fluorescence intensity observed in the absence of DNA and I is the intensity in the presence of DNA. Binding isotherms are presented as plots of Q_{obsd} against the logarithm of the DNA oligomer concentration. The concentration of GR DBD bound to DNA (C_b) was calculated as $C_b = (Q_{obsd}/Q_{max})C_{tot}$, where C_{tot} is the total GR DBD concentration and Q_{max} is the maximum quenching, that is, the quenching observed when all the protein in the sample is bound to DNA. Possible dependencies of Q_{max} on the particular binding state (monomeric or dimeric) of the GR DBD–DNA complex have been discussed (and ruled out) in previous studies (Härd et al., 1990a; Lundbäck et al., 1993).

Analysis of Binding Isotherms. Equilibrium parameters were determined in nonlinear least-squares fits of theoretical binding isotherms to the observed fluorescence quenching as a function of the DNA concentration. A simple one-site model (binding constant K_{obs}) was applied for protein binding to half-site-containing oligomers (one bound protein molecule per DNA oligomer). A two-site cooperative model assuming equal binding affinity for the two half-sites (same binding constant, K_{obs}, as in the one-site model) with an additional cooperativity parameter (ω_{obs}) was used for protein binding to palindromic sites (two protein molecules per oligomer). The models have been described previously (Härd et al., 1990a; Lundbäck et al., 1993). In short, the cooperativity parameter is a measure of the relative change in affinity for protein binding to a second site in a case when the first site is already occupied, i.e., the effective binding constant for this process is $\omega_{obs}K_{obs}$. It is not necessary to consider dimerization of uncomplexed protein molecules because the equilibrium titrations were carried out at low concentrations (~1 μM), whereas NMR studies show that GR DBD protein fragments are still predominantly monomeric at much higher (1 mM) concentrations (Härd et al., 1990b,c; Berglund et al., 1992).

In our previous studies, we encountered a difficulty in obtaining accurate determinations of both ω_{obs} and K_{obs} when fitting these parameters to a single binding isotherm for a titration with a palindromic binding site because the best-fit values of these two parameters are highly correlated, i.e., a high cooperativity with a low binding constant might fit the

curve equally well as a low cooperativity with a high binding constant. In the present study, we determine K_{obs} and ω_{obs} from simultaneous fits of the theoretical binding isotherms for a single half-site and palindromic site equilibria using a "global" value for the binding constant. This procedure avoids most of the uncertainties due to correlated best-fit values and results in a more consistent picture of the two binding processes. This is because the binding constant for binding to a single half-site should (theoretically) be independent on surrounding DNA sequences, whereas any differences in the overall affinity (increase or decrease) due to the presence of two half-sites within a palindromic response element should be reflected in the cooperativity parameter.

The global fitting procedure was not applied in the thermodynamic analysis of GR DBD_{wt} binding to the palGRE2 response element, since the GR DBD_{wt}–GRE2H equilibrium was monitored at one temperature (20 °C) only. In this case, we have instead chosen to determine the product $K_{obs}(\omega_{obs})^{1/2}$, which can be viewed as an effective binding constant for each of the monomers in a dimeric complex (see below). This parameter can be determined directly from the equilibrium isotherms in the following way: It follows from eqs A5 and A6 of Härd et al. (1990) that the free protein concentration at 50% occupancy of available binding sites on palindromic DNA oligomers equals $C_{free} = 1/(K_{obs}(\omega_{obs})^{1/2})$. At these conditions, one also has the relation $C_b = (2C_{DNA})/2 = C_{DNA}$, where C_{DNA} is the total concentration of added palindromic DNA oligomers. The simple relations $C_b = C_{tot}(Q_{obs}/Q_{max})$ and $C_{free} = C_{tot} - C_b$ can then be used to verify that $K_{obs}(\omega_{obs})^{1/2} = 1/(C_{tot} - C_{DNA})$ at this point on the binding isotherm, which can be located using the criterion $C_{DNA} = C_{tot}(Q_{obsd}/Q_{max})$. This graphical method of determining $K_{obs}(\omega_{obs})^{1/2}$ yields results that in all cases differ by less than 20% from the values determined using global fits to half-site and palindromic binding isotherms and less than 0.1 kcal mol^{-1} in the corresponding free energy. Thus, we could confidently use this method to estimate $K_{obs}(\omega_{obs})^{1/2}$ for the GR DBD_{wt}–palGRE2 equilibrium at the temperatures at which half-site binding isotherms were not available.

Errors in the best-fit equilibrium parameters estimated using Monte Carlo simulations (Press et al., 1986), based on estimated standard deviation of individual data points, were found to be very small (<1%) due to high precision of the experimental data. Experimental errors are therefore instead likely to be dominated by uncertainties in measured DNA and protein concentrations. The errors given in Table 1 were estimated from fits of the theoretical binding isotherms to the experimental data assuming total protein and DNA concentrations that were 20% (protein) and 5% (DNA) lower and higher than the experimentally determined concentrations.

Thermodynamic Analysis. The free-energy changes involved in the binding to various half-sites were calculated as $\Delta G^\circ_{obs}{}^{half\text{-}site} = -RT\ln(K_{obs})$, which is the free energy of binding of one protein molecule to a single half-site. To compare the various equilibria for binding to palindromic sites, we use the quantity $\Delta G^\circ_{obs}{}^{dimeric\ site} = -RT\ln(K_{obs}(\omega_{obs})^{1/2}) = -RT\ln(K_{obs}) - {}^1/_2RT\ln(\omega_{obs})$, which can be viewed as an "effective" free-energy change per protein molecule for dimeric binding to a palindromic binding site.

Enthalpy (ΔH) and entropy (ΔS) contributions to measured free energies of binding ($\Delta G = \Delta H - T\Delta S$) were determined in van't Hoff analysis, i.e., by studying the temperature dependence of the equilibrium parameters in the temperature interval 10–35 °C. In Figure 7 we plotted $\ln(K_{obs})$ or $\ln(K_{obs}(\omega_{obs})^{1/2})$ as a function of $1/T$. The slope of such a plot

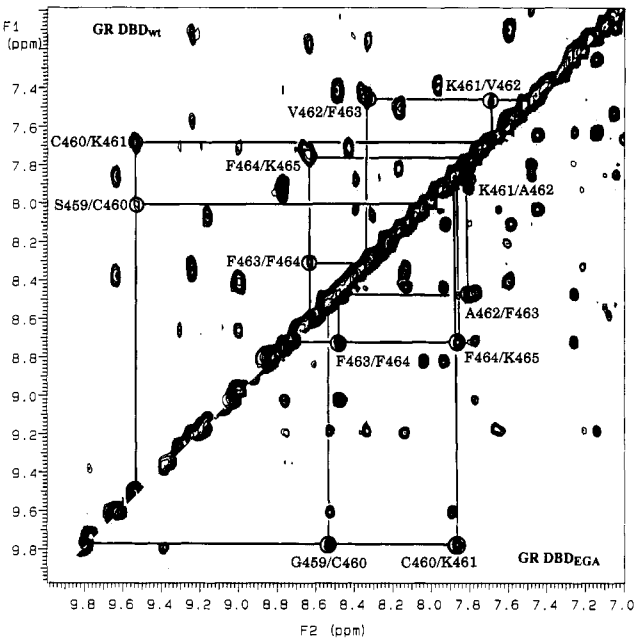

FIGURE 2: Downfield amide regions of NMR NOESY spectra of GR DBD_{wt} (above the diagonal) and GR DBD_{EGA} (below the diagonal). Sequential amide NOE connectivities within the α-helical segment S459–K465 in GR DBD_{wt} and the corresponding segment in GR DBD_{EGA} are indicated.

at any temperature equals $-\Delta H^\circ_{obs}/R$ at that temperature, e.g., $d(\ln(K_{obs}))/d(1/T) = -\Delta H^\circ_{obs}/R$ (the van't Hoff isochore). A non-linear dependence reflects a temperature dependence of ΔH°_{obs}, which is due to a nonzero change in specific heat capacity ($\Delta C_p^\circ{}_{obs}$) upon binding, and this results in compensating enthalpic and entropic contributions to the free-energy change. The temperature dependence of an observed binding constant can in this case be expressed as

$$\ln(K_{obs}) = \frac{\Delta C_p^\circ{}_{obs}}{R}\left[\frac{T_H}{T} - \ln\left(\frac{T_S}{T}\right) - 1\right] \qquad (1)$$

where T_H and T_S are the temperatures at which $\Delta H^\circ_{obs} = 0$ and $\Delta S^\circ_{obs} = 0$, respectively, and $\Delta C_p^\circ{}_{obs}$ is assumed to be temperature independent over the investigated temperature range (Ha et al., 1989).

All binding parameters and thermodynamic quantities referred to in this work are determined on the basis of the total macromolecular concentrations only, neglecting the nonideality of the solution. The determined parameters are therefore only relevant at specific buffer and concentration conditions and are consequently denoted with the subscript "obs" throughout the paper.

RESULTS

Structure of GR DBD_{EGA}. The structure of the triplet mutant GR DBD_{EGA} was studied using NMR spectroscopy. The ^1H NMR spectrum of the mutant is very similar to that of the wild-type protein, indicating similar structures, and small differences in chemical shifts are concentrated to the region of the three mutated residues. Figure 2 shows the amide regions of NOESY spectra of the two proteins. The sequential amide NOE connectivities typical for an α-helical secondary structure are outlined for residues S459–K465 in GR DBD_{wt}, and the corresponding NOE connectivities are also present in the GR DBD_{EGA} spectrum. Other typical NOE connectivities signifying an α-helical conformation of this region can also be found in the NOESY spectrum of GR DBD_{EGA}. One can therefore conclude that the recognition

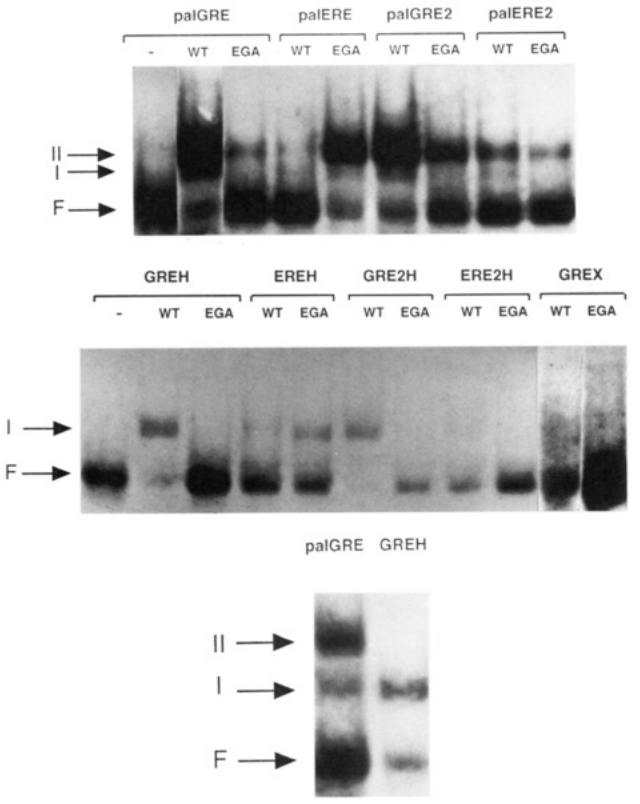

FIGURE 3: (Top) Gel mobility shift assays showing binding of GR DBD_{wt} and GR DBD_{EGA} to the palindromic response elements shown in Figure 1, bottom. Purified protein (3 ng) was added to the solutions used for binding reactions. The lane where no protein was added is marked with a dash. Free DNA oligomers are represented with F, while I and II indicate protein–DNA complexes with one and two proteins bound, respectively. (Middle) Binding of GR DBD_{wt} and GR DBD_{EGA} to the half-site sequences shown in Figure 1 bottom. Purified protein (6 ng) was added to the solutions used for binding reactions. Only one protein–DNA complex (I) can be observed. (Bottom) GR DBD_{wt} binding to the half-site GREH and the corresponding palindromic GRE sequence incorporated in oligonucleotides of the same length (32 bp). The figure illustrates that the protein–DNA complex formed with GREH comigrates with complex I formed with the palindromic GRE.

helix spanning residues G458–E469 of the GR DBD is intact in the mutant protein and that any structural differences between the proteins are to be found on the surface of this helix and in the interactions involving the side chains of the mutated residues.

Gel Mobility Shift Assays. A simple 1:1 stoichiometry for GR DBD_{wt} and GR DBD_{EGA} binding to half-site GRE and ERE sequences is not directly evident from the equilibrium titrations presented below. The possibility of cooperative protein binding to (nonspecific) sites next to the specific half-sites becomes obvious when one considers the cooperative binding of two GR DBD_{wt} or GR DBD_{EGA} to the palindromic GREs and EREs, respectively. Furthermore, the crystal structure of GR DBD in complex with a palindromic GRE with an incorrect (4-bp) half-site spacing reveals a complex where only one of the GR DBD molecules is bound to a specific site and the second protein molecule has chosen to bind cooperatively but nonspecifically (Luisi et al., 1991). On the other hand, the salt conditions used in the equilibrium experiments were carefully chosen in order to minimize nonspecific DNA binding (Härd et al., 1990a; Lundbäck et al., 1993).

We used gel mobility shift assays to firmly establish stoichiometries for GR DBD_{wt} and GR DBD_{EGA} binding to half-site and palindromic DNA oligomers. Figure 3 top, shows protein binding to the palindromic sites included in this study. Two complexes are formed which corresponds to one (complex I) or two (complex II) bound proteins, respectively (Tsai et al., 1988). The relative affinity of the two proteins for the different binding sites agrees well with previous results (Zilliacus et al., 1991). Figure 3, middle, shows protein binding to the corresponding half-site DNA oligomers. Here, only one complex can be observed, and Figure 3, bottom, shows that this complex comigrates with complex I (one protein bound) formed with a palindromic binding sequence incorporated in an oligonucleotide of equal length (32 bp). These observations confirm a 1:1 stoichiometry for GR DBD_{wt} binding to GREH and GRE2H and GR DBD_{EGA} binding to EREH at the temperature and concentrations at which the gel mobility shift assays were carried out (4 °C). One cannot completely exclude other stoichiometries at higher temperatures and concentrations. However, the higher salt concentrations used in the equilibrium titrations can be expected to attenuate the nonspecific binding affinity of GR DBD considerably (Härd et al., 1990a), and we therefore feel confident about the 1:1 stoichiometry for these complexes. However, these gel mobility shift assays do not show whether protein binding to the GREX oligomer and the other low-affinity half-site oligomers is to be considered specific or nonspecific.

It is interesting to note that GR DBD_{EGA} has a low affinity for EREH compared to the affinity of GR DBD_{wt} for GREH (Figure 3, middle) but that the GR DBD_{wt}–palGRE and GR DBD_{EGA}–palERE complexes are formed with similar affinities (Figure 3, top). This effect suggests that there is a difference in the cooperative binding of the proteins, as discussed in more detail below.

Binding to Half-Site-Containing DNA Sequences. Equilibrium titrations of GR DBD_{wt} and GR DBD_{EGA} with the five half-site-containing DNA oligomers (Figure 1, bottom) at 20 °C are shown in Figure 4, top and bottom, respectively. The affinity of GR DBD_{wt} for the various half-sites decreases in the order GREH > GRE2H > EREH ≈ ERE2H > GREX, while the affinity of GR DBD_{EGA} for the same half-sites decreases in the order EREH > GRE2H > ERE2H > GREH > GREX. The affinities of GR DBD_{EGA} for the various half-site oligomers are clearly lower than those of GR DBD_{wt}, in agreement with the gel mobility shift assays (Figure 3). The present results are also in good agreement with those obtained in previous equilibrium titrations (Lundbäck et al., 1993).

The difference in protein binding to GREX compared to the other binding sites indicates some degree of specificity even in the case of protein binding to low-affinity half-sites, such as GR DBD_{wt} to EREH, since the flanking sequences on both sides of the hexameric half-sites are identical in all oligomers studied. However, a closer look at the flanking sequence reveals the presence of a hexameric sequence (GGATCT) which resembles the ERE2H half-site, suggesting that completely nonspecific binding affinity could be lower than the affinity observed for binding to the GREX oligomer. Still, we note that the binding affinity of GR DBD_{wt} for GREX is similar to the binding to calf thymus DNA (Lundbäck et al., 1993), which probably can be considered to be nonspecific in this context. Thus, a comparison of the results from the gel mobility shift assays (Figure 3) and the binding curves for the different binding sites (Figures 4 and 5) shows that some of the fluorescence quenching observed might be due to nonspecific interactions in the case of GR DBD_{wt} binding to EREH, ERE2H, and GREX and GR DBD_{EGA} binding to ERE2H, GREH, and GREX. However, the one-site model

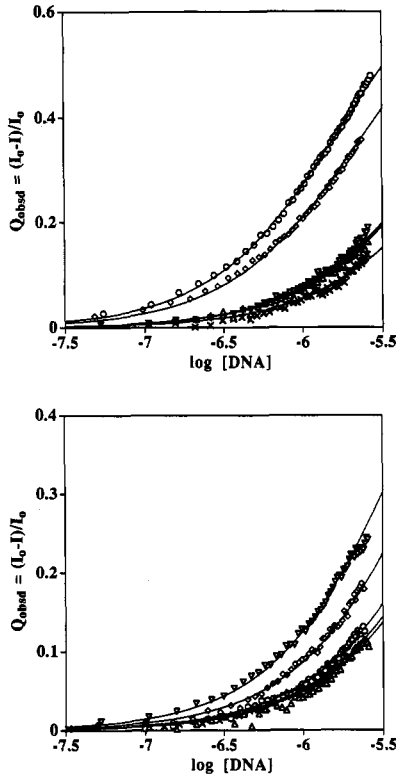

FIGURE 4: (Top) Fractional fluorescence quenching as a function of DNA concentration for reverse titrations of GR DBD_{wt} with (○) GREH, (◇) GRE2H, (△) ERE2H, (▽) EREH, and (×) GREX at constant protein concentration (≈1 μM). The curves represent the best fit of theoretical binding isotherms to experimental data with Q_{max} values according to Table 1. All titrations were performed in 85 mM NaCl, 100 mM KCl, 2 mM $MgCl_2$, 0.3 mM DTT, 0.1 mM $C_{12}E_8$, and 20 mM Tris-HCl at pH 7.4 and a temperature of 20 °C. (Bottom) Fractional fluorescence quenching as a function of DNA concentration for reverse titrations of GR DBD_{EGA} with (○) GREH, (◇) GRE2H, (△) ERE2H, (▽) EREH, and (×) GREX at constant protein concentration (≈1 μM). The curves represent the best fit of theoretical binding isotherms to experimental data with Q_{max} values according to Table 1. Buffer conditions are the same as those given in the legend to Figure 4, top.

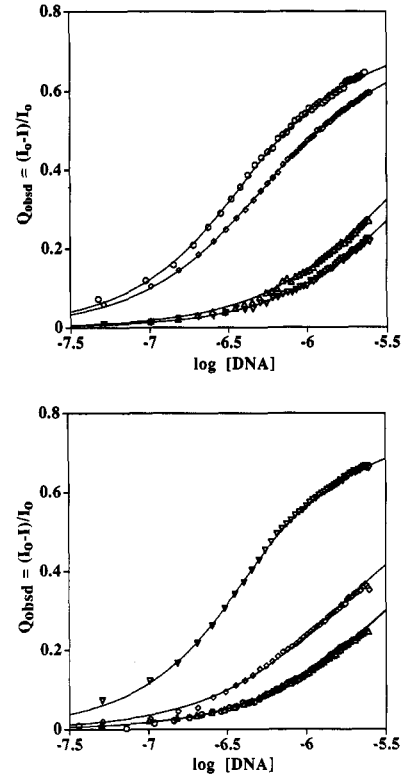

FIGURE 5: (Top) Fractional fluorescence quenching as a function of DNA concentration for reverse titrations of GR DBD_{wt} with (○) palGRE, (◇) palGRE2, (△) palERE2, and (▽) palERE at constant protein concentration (≈1 μM). The curves represent the best fit of theoretical binding isotherms to experimental data with Q_{max} values according to Table 1. Buffer conditions are the same as those given in the legend to Figure 4, top. (Bottom) Fractional fluorescence quenching as a function of DNA concentration for reverse titrations of GR DBD_{EGA} with (○) palGRE, (◇) palGRE2, (△) palERE2, and (▽) palERE at constant protein concentration (≈1 μM). The curves represent the best fit of theoretical binding isotherms to experimental data with Q_{max} values according to Table 1. Buffer conditions are the same as those given in the legend to Figure 4, top.

can still be used to obtain an estimate of the maximum association constants for the corresponding specific complexes (Lundbäck et al., 1993).

In the case of protein binding to half-site DNA oligomers, there is a theoretical possibility of nonspecific cooperative binding of a second protein molecule next to the specifically bound protein. However, the gel mobility shift assay performed at lower salt concentrations confirmed a 1:1 stoichiometry for GR DBD_{wt} binding to GREH and GRE2H and GR DBD_{EGA} binding to EREH. Still, the influence on the fitted parameters of a second protein possibly bound nonspecificity next to a half-site was examined. This was carried out by simultaneously fitting binding curves for palindromic sites and half-sites using three equilibrium parameters: the binding constant for the specific hexameric sequence, the cooperativity parameter, and an additional binding constant reflecting weak binding to a second (nonspecific) site on the half-site oligomer. The fitted values of the specific binding constant and the cooperativity parameter obtained using this three-parameter model were similar to the values obtained using the specific models and in all cases within the error intervals given.

A precise determination of the maximum quenching, Q_{max}, is important for accurate determination of the equilibrium parameters. As discussed previously (Lundbäck et al., 1993), titrations with half-site DNA oligomers cannot be carried out until maximum quenching is observed due to DNA absorbance at 280 nm. In our previous studies, we determined Q_{max} in titrations at slightly lower salt concentrations. Q_{max} values determined in this way were identical (within experimental errors) to the maximum quenching observed for the high-affinity binding to the corresponding palindromic site. In the present study, all the possible palindromic binding sites are included, and precise determinations of the maximum quenching of GR DBD_{wt} and GR DBD_{EGA} fluorescence can be made on the basis of these titrations (Figure 5).

Binding to Palindromic DNA Sequences. Equilibrium titrations of GR DBD_{wt} and GR DBD_{EGA} with the palindromic binding sites (Figure 1, bottom) at 20 °C are shown in Figure 5, top and bottom, respectively. The affinity for the palindromic binding sites is much higher compared to that for single half-sites due to the presence of two half-sites and the effects of positive cooperativity. The affinity of GR DBD_{wt} for the various oligomers decreases in the order palGRE > palGRE2 > palERE2 > palERE, while the affinity of GR DBD_{EGA} for the same DNAs decreases in the order palERE > palGRE2 > palERE2 ≈ palGRE. These results are also in good agreement with those obtained in previous gel mobility shift studies (Zilliacus et al., 1991). Figure 5 also shows that the specificity is completely switched when GR DBD_{wt} is mutated to GR DBD_{EGA}, i.e., the overall affinities of GR DBD_{wt} to palGRE and palERE are very comparable to the

Table 1: Best-Fit Parameters for Sequence-Specific DNA Binding of GR DBD_{wt} and GR DBD_{EGA}[a]

association process[b]	K_{obs} ($M^{-1} \times 10^{-5}$)	ω_{obs}	Q_{max}	$\Delta G°_{obs}$ (kcal mol^{-1}) half-site[c]	$\Delta G°_{obs}$ (kcal mol^{-1}) dimeric site[d]
GR DBD_{wt}–					
GRE	7.6 ± 0.9	10 ± 1	0.76	7.9 ± 0.1	8.6 ± 0.1
GRE2	4.8 ± 0.6	10 ± 2	0.76	7.6 ± 0.1	8.3 ± 0.1
ERE2	1.2 ± 0.2	2 ± 1	0.76	6.8 ± 0.2	7.0 ± 0.2
ERE	1.1 ± 0.2	<1	0.76	6.8 ± 0.2	6.8 ± 0.2
GREX	0.8 ± 0.2		0.76	6.6 ● 0.2	
GR DBD_{EGA}–					
GRE	0.8 ± 0.2	7 ± 2	0.80	6.6 ± 0.2	7.1 ± 0.1
GRE2	1.3 ± 0.2	10 ± 2	0.80	6.9 ± 0.1	7.5 ± 0.1
ERE2	0.7 ± 0.2	14 ± 6	0.80	6.5 ± 0.2	7.3 ± 0.2
ERE	2.2 ± 0.3	121 ± 17	0.80	7.2 ± 0.1	8.6 ± 0.1
GREX	0.7 ± 0.2		0.80	6.5 ± 0.2	
GR DBD_{wt}–GRE (°C)					
10	4.5 ± 0.5	9 ± 2	0.77	7.3 ± 0.1	7.9 ± 0.1
15	5.4 ± 0.6	9 ± 2	0.77	7.6 ± 0.1	8.2 ± 0.1
20	7.6 ± 0.9	10 ± 1	0.76	7.9 ± 0.1	8.6 ± 0.1
25	9.8 ± 1.2	10 ± 2	0.74	8.2 ± 0.1	8.8 ± 0.1
30	10.9 ± 1.4	13 ± 1	0.74	8.4 ± 0.1	9.1 ± 0.1
35	10.6 ± 1.3	17 ± 1	0.74	8.5 ± 0.1	9.4 ± 0.1
GR DBD_{wt}–GRE2 (°C)					
10			0.77		7.9 ± 0.1[e]
15			0.77		8.1 ± 0.1[e]
20	4.8 ± 0.6	10 ± 2	0.76	7.6 ± 0.1	8.3 ± 0.1
25			0.74		8.4 ± 0.2[e]
30			0.74		8.7 ± 0.1[e]
35			0.74		8.8 ± 0.2[e]
GR DBD_{EGA}–ERE (°C)					
10	1.5 ± 0.2	118 ± 17	0.81	6.7 ± 0.1	8.0 ± 0.1
15	1.8 ± 0.3	114 ± 17	0.81	6.9 ± 0.2	8.3 ± 0.1
20	2.2 ± 0.3	121 ± 17	0.80	7.2 ± 0.1	8.6 ± 0.1
25	2.5 ± 0.3	138 ± 9	0.80	7.4 ± 0.1	8.8 ± 0.1
30	2.9 ± 0.4	125 ● 8	0.80	7.6 ± 0.1	9.0 ± 0.1
35	3.4 ± 0.4	85 ± 7	0.79	7.8 ± 0.1	9.2 ± 0.1

[a] Uncertainties given result from uncertainties in protein (20%) and DNA (5%) concentration. [b] If not given, a temperature of 20 °C was used. [c] Calculated as $RT\ln(K_{obs})$. [d] Calculated as $RT\ln(K_{obs}(\omega_{obs})^{1/2})$. Refer to the text for a discussion on the physical meaning of this entity. [e] The effective binding constant ($K_{obs}(\omega_{obs})^{1/2}$) is the only parameter evaluated (no half-site data).

corresponding affinities of GR DBD_{EGA} to palERE and palGRE.

Fitted association constants and cooperativity parameters obtained in simultaneous fits of half-site and palindromic site experimental data are listed in Table 1 together with the corresponding free energies of association ($\Delta G°_{obs}{}^{\text{half-site}} = -RT\ln(K_{obs})$) and the free energy associated with the binding of each of the two monomers in a dimeric complex ($\Delta G°_{obs}{}^{\text{dimeric site}} = -RT\ln(K_{obs}(\omega_{obs})^{1/2})$). The difference in cooperativity for GR DBD_{wt} and GR DBD_{EGA} binding to DNA observed in the gel mobility shift analysis is apparent in the quantification of the equilibrium titrations. There are clearly stronger protein–protein interactions involved when the mutant GR DBD_{EGA} binds to palERE.

In a previous paper (Lundbäck et al., 1993), we reported a somewhat larger value for the cooperativity parameter, ω_{obs} = 25–50, in the case of GR DBD binding to palGRE. This value was estimated without the use of a global binding constant which caused severe problems with the correlation between fitted parameters. Furthermore, the titrations were performed at slightly different buffer conditions using a different titration procedure with a lower precision and included the binding to a single palindromic site at one temperature only. We therefore feel confident about the cooperativity parameters reported here.

Thermodynamic Analysis. The thermodynamic driving forces involved in the sequence-specific binding were determined by means of van't Hoff analysis. The thermodynamics were evaluated for binding of GR DBD_{wt} to the GREH, palGRE, and palGRE2 DNA oligomers and for binding of GR DBD_{EGA} to the EREH and palERE oligomers. Figure 6, top, shows binding isotherms for binding of GR DBD_{wt} to GREH at several temperatures between 10 and 35 °C. The observed temperature dependence is common to all five binding processes studied here: the binding affinity is low at low temperatures (10 °C), increases with temperature, and levels off at higher temperatures (35 °C), indicating that the association reaction is entropy driven (positive enthalpy of association) within this temperature interval.

Figure 6, bottom, shows binding isotherms for GR DBD_{wt} binding to palGRE and palGRE2 at 10 and 35 °C. It is evident that GR DBD_{wt} binds stronger to palGRE than to palGRE2 at both temperatures. It is also interesting to note that the temperature dependence of the GR DBD_{wt}–palGRE2 equilibrium is smaller than that of the GR DBD_{wt}–palGRE equilibrium. This observation indicates that the enthalpy of association is more favorable for the weaker (palGRE2) complex in the temperature interval studied. This more favorable enthalpy is evidently overcompensated by entropic effects which result in a stronger overall binding affinity for palGRE. The possible molecular basis and implications of this entropy-driven binding-site specificity are discussed below.

Equilibrium parameters for the various complexes as a function of temperature were determined as described above, and the results are summarized in Table 1 together with the corresponding free-energy changes. In the case of GR DBD_{wt} binding to palGRE2, there is no corresponding temperature study of the binding to GRE2H, which means that a simultaneous fit of a global binding constant to half-site and palindromic site experimental data could not be carried out

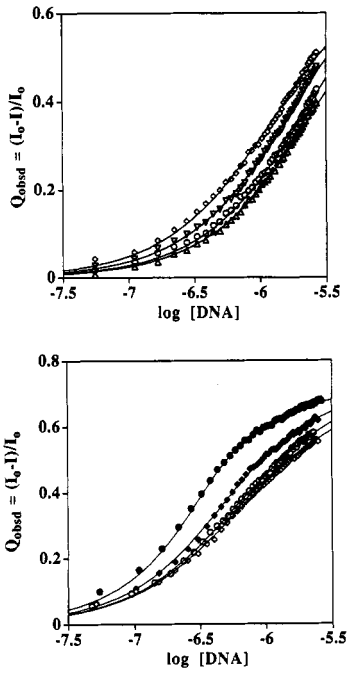

FIGURE 6: (Top) Fractional fluorescence quenching as a function of DNA concentration for reverse titrations of GR DBD_{wt} with palGRE at (△) 10, (○) 15, (▽) 20, and (◇) 35 °C at constant protein concentration (≈1 μM). The curves represent the best fit of theoretical binding isotherms to experimental data with Q_{max} values according to Table 1. Buffer conditions are the same as those given in the legend to Figure 4, top. (Bottom) Fractional fluorescence quenching as a function of DNA concentration for reverse titrations of GR DBD_{wt} with palGRE (○) and palGRE2 (◇) at 10 °C (open) and 35 °C (filled) at constant protein concentration (≈1 μM). The curves represent the best fit of theoretical binding isotherms to experimental data with Q_{max} values according to Table 1. Buffer conditions are the same as those given in the legend to Figure 4, top.

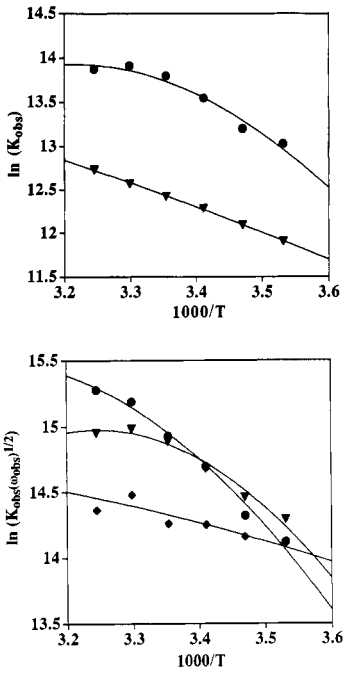

FIGURE 7: (Top) van't Hoff plot of $\ln(K_{obs})$ versus $1/T$ for GR DBD_{wt} binding to GREH (●) and for GR DBD_{EGA} binding to EREH (▼). The curves represent the best fit of estimated association constants to eq 1. (Bottom) van't Hoff plot of $\ln(K_{obs}(\omega_{obs})^{1/2})$ versus $1/T$ for GR DBD_{wt} binding to palGRE (●) and palGRE2 (◆) and for GR DBD_{EGA} binding to palERE (▼). The curves represent the best fit of estimated equilibrium parameters to eq 1.

in this case. However, the problem of high correlation between the binding constant and the cooperativity parameter can to some extent be avoided through the determination of the effective binding constants ($K_{obs}(\omega_{obs})^{1/2}$), as discussed above, and the thermodynamics for the GR DBD_{wt}–GRE and GR DBD_{wt}–GRE2 complexes can be compared on the basis of the free energies ($\Delta G°_{obs}{}^{\text{dimeric site}} = -RT \ln(K_{obs}(\omega_{obs})^{1/2})$).

van't Hoff plots (Figure 7) of the five equilibria reveal a nonlinear dependency of $\ln(K_{obs})$ or $\ln(K_{obs}(\omega_{obs})^{1/2})$ as a function of $1/T$, indicating a negative $\Delta C_p°_{obs}$ upon formation of the complexes, although this behavior is less pronounced in the case of GR DBD_{EGA} binding to an ERE half-site. The results of three-parameter ($\Delta C_p°_{obs}$, T_H, T_S) fits of eq 1 to the association constants (K_{obs}) and effective binding constants for dimeric binding ($K_{obs}(\omega_{obs})^{1/2}$) are shown in Table 2, and the corresponding temperature dependencies in $\Delta H°_{obs}$ and $\Delta S°_{obs}$ [calculated according to Ha et al. (1989)] are shown in Figure 8. It is evident from Table 2 that the uncertainties in T_H and T_S in some cases are rather large. However, the qualitative differences in the nature of thermodynamic driving forces driving the various association processes studied are obvious in the van't Hoff plots (Figure 7).

The heat capacity effect accompanying noncovalent processes involving globular proteins can to some extent be calibrated in terms of dehydration of nonpolar and polar surfaces upon complexation (Spolar et al., 1992). We previously measured a very large $\Delta C_p°_{obs}$ for the binding of GR DBD_{wt} to the GREH half-site and concluded that this could not be fully accounted for by the simple relation given by Ha et al. (1989). In the present studies, where improvements in methodology allow us to increase the precision of determined equilibrium parameters, we find that the $\Delta C_p°_{obs}$ for this equilibrium probably is smaller than the previously

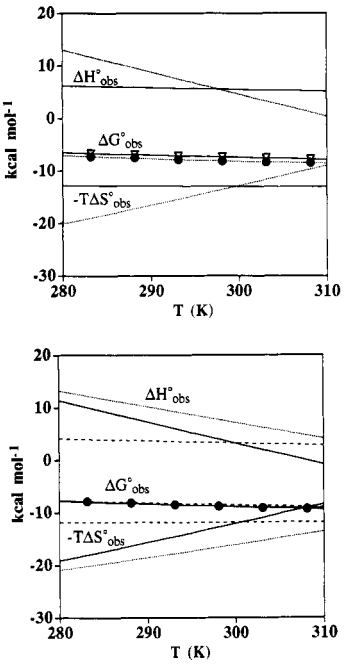

FIGURE 8: (Top) Thermodynamics of the GR DBD_{wt}–GREH (···) and GR DBD_{EGA}–EREH (—) association processes. Both binding processes are entropy driven in the studied temperature interval. Determined $\Delta G°_{obs}$ values for GR DBD_{wt} binding to GREH (●) and for GR DBD_{EGA} binding to EREH (▽) are also indicated. (Bottom) Thermodynamics of the GR DBD_{wt}–GRE (···), GR DBD_{wt}–GRE2 (– – –), and GR DBD_{EGA}–ERE (—) binding processes. All the binding processes are entropy driven in the temperature interval studied, although shifts in the nature of thermodynamic driving forces at higher temperatures are evident. Determined $\Delta G°_{obs}$ values for GR DBD_{wt} binding to GRE (●) are also indicated.

Table 2: Best-Fit Thermodynamic Parameters Estimated for Sequence-Specific DNA Binding of GR DBD_{wt} and GR DBD_{EGA}[a]

association process	$\Delta C_p^{\circ}{}_{obs}$ (kcal mol^{-1} $K^{<-1}$)	T_H (K)	T_S (K)
GR DBD_{wt} + GREH ⇒ complex	−0.42 ± 0.27	311 ± 77	nd[b]
2 GR DBD_{wt} + palGRE ⇒ complex	−0.60 ± 0.18	324 ± 15	359 ± 47
2 GR DBD_{wt} + palGRE2 ⇒ complex	−0.06 ± 0.50	373 ± 104	nd[b]
GR DBD_{EGA} + EREH ⇒ complex	−0.04 ± 0.17	455 ± 144	nd[b]
2 GR DBD_{EGA} + palERE ⇒ complex	−0.80 ± 0.20	308 ± 4	332 ± 13

[a] Errors given are estimated from Monte Carlo simulations. [b] Not determined.

reported value (Table 2), resulting in better agreement with predictions based on surface area calculations.

DISCUSSION

The thermodynamics of DNA–protein interactions are a challenging area of biophysics, which presently is receiving an increasing degree of attention [see, for instance, Lesser et al. (1993), Takeda et al. (1992), and Ha et al. (1989, 1992)]. The underlying problem, to understand the molecular mechanisms of sequence discrimination upon DNA binding, has not yet been solved for any specific DNA–protein complex. It is not straightforward how to analyze a single DNA–protein structure with regard to the importance of various observed interactions for two major reasons. First, although it might be possible to draw conclusions about interaction energies, i.e., the enthalpy component of the binding constant, it is not possible to deduce anything about the entropy component of the binding constant. Second, the effect of an alteration in DNA and/or protein sequence is difficult to predict because the system might respond to a mutation by significantly altering the structure, e.g., by unexpectedly giving up some specific interactions and making new ones that are not observed in the original structure. Such responses, which can take a multitude of forms, might perhaps be simulated, but theoretical methods can still not be considered accurate enough to reproduce interaction free energies of the order of 1 kcal mol^{-1} or less. Thus, to successfully investigate the origin of sequence specificity in a DNA–protein complex, one should ideally determine not only one but several structures which all contain minor variations in terms of mutations that change the specificity of the protein and/or altered DNA-binding site sequences. These structure determinations should then be complemented by thermodynamic analysis of the various complexes to investigate the energetics, and all available information should be compiled and rationalized in the context of the native complex. A complete analysis probably also requires an account of the release of water molecules and ions upon complex formation (Ha et al., 1992, and references therein).

Regarding the binding of the GR and ER DBDs to the (similar) GRE and ERE sequences, there has been substantial progress on the structural level by the determination of a GR DBD–GRE complex (Luisi et al., 1991) and the recent determination of an ER DBD–ERE complex (Schwabe et al., 1993). Additional related structures are presently studied in the laboratory of Dr. Paul Sigler, including the structure of a GR DBD mutant (very similar to the mutant GR DBD_{EGA} studied here) in a complex with an ERE response element (Dr. Dan Gewirth, Univ. of Chicago, personal communication).

The present paper represents an additional step in the complementary thermodynamic analysis of the DNA binding by the GR and ER DBDs. We have determined free energies of association at 20 °C for the binding of the wild-type GR DBD_{wt} and the mutant GR DBD_{EGA} to four related response elements. We have in all cases been able to determine the contribution due to cooperative binding by comparing binding to half-site and palindromic DNA oligomers. In addition, we have investigated the thermodynamics for the five strongest complexes using van't Hoff analyses.

Discrimination between GRE and ERE Sequences. It was previously shown that mutation of three residues in the GR DBD_{wt} to create the GR DBD_{EGA} mutant resulted in an altered DNA-binding specificity, such that it had a higher affinity for an ERE compared to a GRE, according to gel mobility shift assays (Zilliacus et al., 1991). The present equilibrium studies provide a quantification of these observations in terms of free-energy changes upon binding. We noted above that the loss in DNA-binding affinity for the palGRE-binding site due to the triple mutation introduced in the GR DBD_{EGA} is completely compensated by changing the palGRE sequence to a palERE sequence. However, it is interesting to note that the altered specificity is not completely due to different binding constants for the various sites but that the GR DBD_{EGA} binds strongly to the ERE sequence because protein–protein interactions (cooperative binding) are enhanced considerably compared to those in the GR DBD_{wt}–GRE complex. Thus, it seems that the two proteins use somewhat different binding modes in binding to the palGRE and palERE sequences, respectively. In other words, there are structural differences between the two complexes, which are not direct consequences of altered interactions between functional groups on the interacting surfaces within an otherwise fixed structural framework. The effect is not completely unexpected in view of the differences between the structures of the GR DBD–GRE and ER DBD–ERE complexes (the recognition helices of the GR DBD_{EGA} and the ER DBD are very similar), where there is a considerable rearrangement of side chains at the DNA–protein interface (Schwabe et al., 1993). One might therefore also expect minor differences in the orientation of the bound proteins in the two cases, resulting in different interactions at the protein–protein interface.

Binding to the palGRE2 sequence by the two proteins represents an interesting intermediate case. The GR DBD_{wt} has a lower affinity for the GRE2 than for the GRE, whereas GR DBD_{EGA} shows the opposite behavior. The cooperativity is similar in all four complexes, indicating that the overall structural differences between the complexes are not as large as when comparing binding to a GRE versus an ERE. Thus, it seems that mutation of the AT base pair at position 4 (Figure 1, bottom) might not result in significantly altered binding modes. The stronger binding of GR DBD_{EGA} to a GRE2- compared to a GRE-binding site is probably due to direct interactions of the Glu458 with the cysteine base as discussed by Luisi et al. (1991) and Zilliacus et al. (1991, 1992) and as observed in the ER DBD–ERE complex (Schwabe et al., 1993). The weaker binding of GR DBD_{wt} to a GRE2 compared to a GRE is more difficult to rationalize in structural terms, but the thermodynamics of this sequence specificity actually provide some clues, as discussed below.

Thermodynamically Different Association Processes. There are significant differences in thermodynamics between GR DBD_{wt} binding to palGRE and GR DBD_{EGA} binding to palERE (Figure 8, bottom). The formation of both complexes is entropy driven in the temperature interval 10–35 °C, but $\Delta H°_{obs}$ is more favorable in the case of GR DBD_{EGA} binding to palERE. This difference is compensated by a less favorable $\Delta S°_{obs}$, resulting in almost identical overall binding affinities in the two cases. It is interesting (and speculative) to note that the differences in thermodynamics correlate with the number of specific DNA–protein interactions as well as the number of strongly bound water molecules observed in the GR and ER DBD complexes with a GRE and ERE, respectively (although it should be noted that the GR DBD_{EGA} mutant used in this study is different from the ER DBD used in the structural studies). The ER complex involves a larger number of direct and water-mediated protein–DNA interactions than the GR complex, which, in principle, is consistent with a more favorable interaction energy. The larger number of bound waters in the ER complex might then also account for the less favorable $\Delta S°_{obs}$ upon binding because each water molecule that is released from a surface can be expected to give a favorable entropy contribution to complex formation. Still, it should be emphasized that this interpretation has to be confirmed by at least one more structure determination, preferably of a GR DBD_{EGA}–ERE complex. We also note that our interpretation does not hold for the binding of the two proteins to the half-site ERE and GRE sequences, although these thermodynamic data, which are based on best-fit K_{obs} values, are less firm than the thermodynamic data for binding to the palindromic DNAs, which are based on the more accurately determined $K_{obs}(\omega_{obs})^{1/2}$ parameter. Another possible scenario is that the different thermodynamics in the two cases are related to protein–protein interactions rather than to protein–DNA interactions.

A Case of Entropy-Driven DNA-Binding Specificity. The temperature dependence of the binding of GR DBD_{wt} to palGRE and palGRE2 is illustrated in Figure 7, bottom. The affinity for palGRE2 is clearly lower at all investigated temperatures. Still, it is evident from the slopes of the two van't Hoff plots that the $\Delta H°_{obs}$ in this temperature range is less favorable in the case of GR DBD_{wt} binding to palGRE. This fact is further illustrated in Figure 8, bottom, where the thermodynamical parameters are plotted against temperature. The preference of GR DBD_{wt} for the palGRE compared to the palGRE2 sequence is therefore entropy driven, i.e., the unfavorable $\Delta(\Delta H°_{obs})$ for the formation of a GR DBD_{wt}–palGRE complex instead of a GR DBD_{wt}–palGRE2 complex is overcompensated by a favorable $\Delta(\Delta S°_{obs})$. This behavior is in contrast to a commonly held view that sequence specificity is a result of favorable interaction energies in a "direct readout" mechanism, where the interaction energy due to hydrogen bonds and van der Waals contacts is optimized (ΔH minimized) in the strongest binding sites. It has been known for some time that the formation of DNA–protein complexes can be entropy driven (Ha et al., 1989, and references therein). The present case shows that entropy effects can play a major role in sequence specificity as well.

Molecular modeling of the GR DBD–GRE complex (Luisi et al., 1991) provides some insight into the molecular mechanism for the observed thermodynamics. The difference between the GRE and GRE2 is that an AT base pair at position 4 in the former is replaced by a CG base pair in the latter. The consequences for the surface of the DNA major groove are not very large: The bulky methyl group of the thymine is removed, and the interbase hydrogen-bonding carbonyl and amino groups of the AT base pair are switched in the CG base pair. The origin of the entropy-driven specificity in GR DBD_{wt} binding to GRE, but favorable enthalpy in the case of binding to GRE2, might be a consequence of the removal of the thymine methyl which creates a cavity between the interacting surfaces. The cavity could possibly be filled with an additional (immobilized) water molecule, which in this position might form hydrogen bonds with the cytosine carbonyl and another strongly bound water used in a water-mediated contact between Lys461 and the cytosine at position 5 of the GRE. This process could be entropically unfavorable due to the immobilization of an extra water molecule but energetically favorable due to the formation of two additional hydrogen bonds. Alternatively, the protein might reorient itself in the binding site or direct a neighboring side chain to fill the cavity. However, this mechanism seems less likely because the closest GR DBD residue is Gly458, and the other somewhat more distant side chains Val462 and Lys461 are probably needed to make specific contacts with surrounding base pairs at positions 3 and 5, respectively, to retain overall binding affinity.

ACKNOWLEDGMENT

We thank M.Sc. Mats Eriksson for assistance in the calculation of solvent-accessible surface areas, Helena Berglund for NMR sample preparations, and Drs. Daniela Rhodes and John W. R. Schwabe at the MRC, University of Cambridge, for communicating their results on the structure of the ER DBD–ERE complex prior to publication.

REFERENCES

Baumann, H., Paulsen, K., Kovács, H., Berglund, H., Wright, A. P. H., Gustafsson, J.-A., & Härd, T. (1993) *Biochemistry 32*, 13463–13471.

Beato, M. (1989) *Cell 56*, 335–344.

Berglund, H., Dahlman-Wright, K., Kovács, H., Gustafsson, J.-A., & Härd, T. (1992) *Biochemistry 31*, 12001–12011.

Birdsall, B., King, R. W., Wheeler, M. R., Lewis, C. A., Goode, S. R., Dunlap, R. B., & Roberts, G. C. K. (1983) *Anal. Biochem. 132*, 353–361.

Botuyan, M. V., Keire, D. A., Kroen, C., & Gorenstein, D. G. (1993) *Biochemistry 32*, 6863–6874.

Brenowitz, M., Jamison, E., Majumdar, A., & Adhya, S. (1990) *Biochemistry 29*, 3374–3383.

Cantor, C. R., & Schimmel, P. R. (1980) *Biophysical Chemistry*, Part II, Freeman, San Francisco.

Dahlman-Wright, K., Siltala-Roos, H., Carlstedt-Duke, J., & Gustafsson, J.-A. (1990) *J. Biol. Chem. 265*, 14030–14035.

Danielsen, M., Hinck, L., & Ringold, G. M. (1989) *Cell 57*, 1131–1138.

Evans, R. M. (1988) *Science 240*, 889–895.

Fried, M., & Crothers, D. M. (1981) *Nucleic Acids Res. 9*, 6505–6525.

Griesinger, C., Otting, G., Wüthrich, K., & Ernst, R. R. (1988) *J. Am. Chem. Soc. 110*, 7870–7872.

Ha, J.-H., Spolar, R. S., & Record, M. T., Jr. (1989) *J. Mol. Biol. 209*, 801–816.

Ha, J.-H., Capp, M. W., Hohenwalter, M. D., Baskerville, M., & Record, M. T., Jr. (1992) *J. Mol. Biol. 228*, 252–264.

Härd, T., & Gustafsson, J.-A. (1993) *Acc. Chem. Res. 26*, 644–650.

Härd, T., Dahlman, K., Carlstedt-Duke, J., Gustafsson, J.-A., & Rigler, R. (1990a) *Biochemistry 29*, 5358–5364.

Härd, T., Kellenbach, E., Boelens, R., Maler, B. A., Dahlman, K., Freedman, L. P., Carlstedt-Duke, J., Yamamoto, K. R., Gustafsson, J.-A., & Kaptein, R. (1990b) *Science 249*, 157–160.

Härd, T., Kellenbach, E., Boelens, R., Kaptein, R., Dahlman, K., Carlstedt-Duke, J., Freedman, L. P., Maler, B. A., Hyde, E. I., Gustafsson, J.-A., & Yamamoto, K. R. (1990c) *Biochemistry 29*, 9015–9023.

Klock, G., Strähle, U., & Schütz, G. (1987) *Nature 329*, 734–736.

Lesser, D. R., Kurpiewski, M. R., Waters, T., Connolly, B., & Len-Jacobson, L. (1993) *Proc. Natl. Acad. Sci. U.S.A. 90*, 7548–7552.

Luisi, B. F., Xu, W. X., Otwinowski, Z., Freedman, L. P., Yamamoto, K. R., & Sigler, P. B. (1991) *Nature 352*, 497–505.

Lundbäck, T., Cairns, C., Gustafsson, J-A., Carlstedt-Duke, J., & Härd, T. (1993) *Biochemistry 32*, 5074–5082.

Macura, S., & Ernst, R. R. (1980) *Mol. Phys. 41*, 94–117.

Mader, S., Kumar, V., de Verneuil, H., & Chambon, P. (1989) *Nature 338*, 271–274.

Mahler, H. R., Kline, B., & Mehrota, B. D. (1964) *J. Mol. Biol. 9*, 801–811.

Parker, M. G., Ed. (1991) *Nuclear Hormone Receptors*, Academic Press, London.

Press, W. H., Flannery, B. P., Teukolsky, S. A., & Vetterling, W. T. (1986) in *Numerical Recipes*, Chapter 14, Cambridge University Press, Cambridge, England.

Record, M. T., Jr., Ha, J.-H., & Fisher, M. A. (1991) *Methods Enzymol. 208*, 291–343.

Schwabe, J. W. R., Neuhaus, D., & Rhodes, D. (1990) *Nature 348*, 458–461.

Schwabe, J. W. R., Chapman, L., Finch, J. T., & Rhodes, D. (1993) *Cell 75*, 567–578.

Spolar, R. S., Livingstone, J. R., & Record, M. T., Jr. (1992) *Biochemistry 31*, 8382–8385.

Strähle, U., Klock, G., & Schütz, G. (1987) *Proc. Natl. Acad. Sci. U.S.A. 84*, 7871–7875.

Takeda, Y., Ross, P. D., & Mudd, C. P. (1992) *Proc. Natl. Acad. Sci. U.S.A. 89*, 8180–8184.

Tsai, S. Y., Carlstedt-Duke, J., Weigel, N. L., Dahlman, K., Gustafsson, J.-A., Tsai, M.-J., & O'Malley, B. W. (1988) *Cell 55*, 361–369.

Umesono, K., & Evans, R. M. (1989) *Cell 57*, 1139–1146.

Zilliacus, J., Dahlman-Wright, K., Wright, A., Gustafsson, J.-A., & Carlstedt-Duke, J. (1991) *J. Biol. Chem. 266*, 3101-3106.

Zilliacus, J., Wright, A. P. H., Norinder, U., Gustafsson, J.-A., & Carlstedt-Duke, J. (1992) *J. Biol. Chem. 267*, 24941–24947.